Geofísica Internacional (2015) 54-1: 95-109

Original paper

Evaluation of soil liquefaction from surface analysis

Efraín Ovando Shelley, Vanessa Mussio*, Miguel Rodríguez and José G. Acosta Chang

Received: March 31, 2014; accepted: May 21, 2014; published on line: December 12, 2014

Resumen

En este artículo describimos cómo estimar el potencial licuable de arenas con algunas técnicas para estimar perfiles de velocidad de onda de corte obtenidos midiendo vibraciones ambientales y a partir de ondas generadas artificialmente. Las mediciones se realizan con facilidad, consumen poco tiempo y además resultan más baratas que otras técnicas. El método pasivo de Análisis de Microtremores (MAM) y el activo de Análisis Multicanal de Ondas Superficiales (MASW) se comenzaron a usar recientemente en estudios de licuación de arenas. En el trabajo se describe un método que se empleó en el Valle de Mexicali para caracterizar el suelo en términos de su velocidad de onda de corte con el fin de evaluar el potencial de licuación. Nuestros resultados demuestran las ventajas del método propuesto.

Palabras clave: Método pasivo de análisis de microtremores (MAM), Método de Análisis Multicanal de Ondas Superficiales.

Abstract

In this paper we describe how some techniques for estimating shallow shear wave velocity profiles obtained from measurements of ambient vibrations and from artificially generated waves can be used to assess sand liquefaction potential. The measurements are easy, quick and more economical than most other methods. The passive Microtremor Analysis Method (MAM) and the active Multichannel Analysis of Surface Waves (MASW) have only recently been adopted for liquefaction studies. We propose a method that was applied in the valley of Mexicali to characterize soil in terms of shear wave velocity to assess liquefaction potential; our results display its advantages.

Keywords: Microtremor Analysis Method (MAM), active Multichannel Analysis of Surface Waves (MASW), sand liquefaction, liquefaction potential

E. Ovando Shelley
V. Mussio*
M. Rodríguez
Instituto de Ingeniería
Universidad Nacional Autónoma de México
Ciudad Universitaria
Delegación Coyoacán, 04510
México D.F., México
*Corresponding author: vanessamussio@gmail.com

J. G. Acosta Chang
Centro de Investigación Científica y Educación Superior de Ensenada.

Introduction

Many authors have described and studied liquefaction of granular soils (Seed *et al*.1971; Poulos *et al.* 1985; Ishihara K. 1993). It occurs when vibrations or water pressure within soil cause the solid particles to cease having contact with one another. This condition is generally caused by the passage of seismic waves through loose or very loose saturated sandy soils. The soil behaves temporarily as a liquid and loses its ability to support weight. Sand boils, ground fissures or lateral spreading are typical manifestations of sand liquefaction (Marcuson, 1978).

Shear wave velocity (V_s) has been correlated with cyclic stress ratio to assess soil liquefaction potential. V_s is estimated from cross-hole or down-hole seismic surveys (Stokoe and Narzian, 1985; Tokimatsu et al., 1990; Kanyen *et al.*, 1992; Andrus and Stokoe, 1997; Yu Shizhou, *et al.*, 2008). In this paper we present a method in which shear wave velocity profiles are derived from Microtremor Analysis Method (MAM) and from Multichannel Analysis of Surface Waves (MASW). Combining MAM and MASW allowed us to reach a deeper penetration depth. Specifically, higher frequency waves generated by sledgehammer impacts travel through shallower depths and can be combined with lower frequency data from microtremors that travel through greater depths. The procedure also clarifies modal trends (Park *et al*., 2007).

We applied a combination of both techniques to a site in the Mexicali Valley, Baja California, in an area of high seismicity and high population density. Sand liquefaction has repeatedly affected Mexicali, the largest city in the region, causing extensive damage there and in towns and villages as well as in canals, roads and other facilities.

Study area

Location

Mexicali is a border city that accounts for 18% of the surface of the state of Baja California. It is bounded on the north by the city of Calexico, California, USA. The site we studied is located in the Solidaridad Social Township, 5 km south of downtown Mexicali and about 10 km south of the border (Figure 1), along a bend in an affluent of the Colorado River.

The Mexicali Valley is within the Colorado River delta. Geologically young sandy sediments are present over the delta region. High groundwater levels and strong ground motions combined to bring about extensive liquefaction in the El Mayor-Cucapah earthquake of April 4, 2010, the largest earthquake to strike this area since 1892. It was possibly larger than the 1940 earthquake (M_w= 6.9) or any of the early 20th century events in northern Baja California. It had a magnitude 7.2 M_w with epicenter on the western margin of the Mexicali Valley where the El Major and Cucapah faults converge, some 40 km south of the Mexicali urban area.

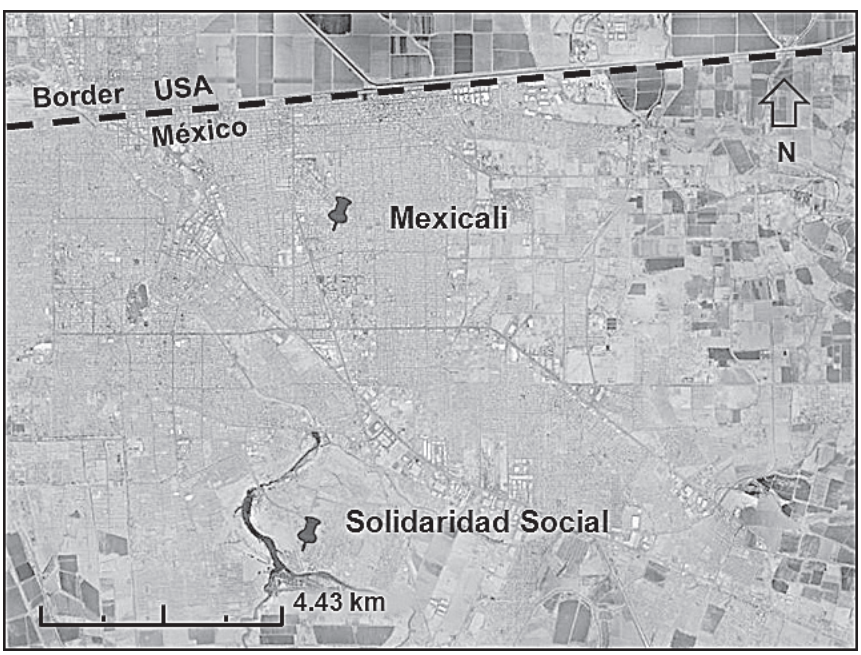

Figure 1. Solidaridad Social township location.

Superficial cracks and fractures appeared along the riverbanks (Figure 2). The main fracture was 1726 m long and secondary cracks extended to about 800 m. Severe economic damage occurred to homes, the canal system and roadways. At least 151 homes suffered some degree of damage associated with the earthquake, including fissures and differential settlements (INDIVI, 2010). Earthquake induced liquefaction, lateral spreading, sand boils and flooding occurred extensively across farm lands and along rivers and irrigation canals.

Liquefaction potential: simplified empirical analysis

Three parameters are needed to assess liquefaction potential using the simplified empirical method: a) shear velocity V_s; b) the cyclic stress ratio (CSR) and c) the capacity of the soil to resist liquefaction, expressed in terms of the cyclic resistance ratio (CRR). Shear wave velocity is proportional to soil stiffness and in the simplified method, it must be corrected to account for the effect of overburden stress (V_{s1}). Our procedure incorporates some updates and improvements to the original simplified method (Youd *et al*., 2001).

For the calculation of the cyclic stress ratio, $\frac{\tau_c}{\sigma'_v}$, we use an expression from the original method:

$$\frac{\tau c}{\sigma'_v} \approx 0.65 \frac{a_{\max}}{g} \frac{\sigma_v}{\sigma'_v} r_d \qquad (1)$$

where a_{max} is the maximum horizontal acceleration at the surface of the soil; is the acceleration of gravity; σ_v and σ'_v are the total and effective vertical stresses respectively and r_d is the coefficient of reduction of efforts. The following equations may be used to estimate average values of r_d (Liao *et al*., 1988; Robertson and Wride, 1998).

$$r_d = 1.0 - 0.00765 z \; for \; z \leq 9.15m \qquad (2)$$

$$r_d = 1.174 – 0.0267 z \; for \; z \; 9.15 \; m < z \leq 23m \qquad (3)$$

where z is the depth below ground surface (m)

The cyclic resistance ratio, CRR, is used to set apart well-characterized sites where liquefaction occurred from those where it did not. Well-characterized sites are those where the stratigraphy is known and where field penetration resistance is available, commonly, usually from SPT or CPT tests (Figure 3). Andrus and Stokoe (1997, 2000) developed liquefaction resistance criteria from 26 earthquakes and shear wave velocities measured in the field at 70 sites (Figure 4). The curve in that figure was obtained from field observations after earthquakes with M_w=7.5, from the results of Vs measurements and from estimations of the cyclic stress ratio (equation 1). Their empirical CRR curve in Figure 4 separates the points in the CSR versus V_{s1} space where liquefaction did and did not occur.

Figure 2. Superficial cracks and fractures.

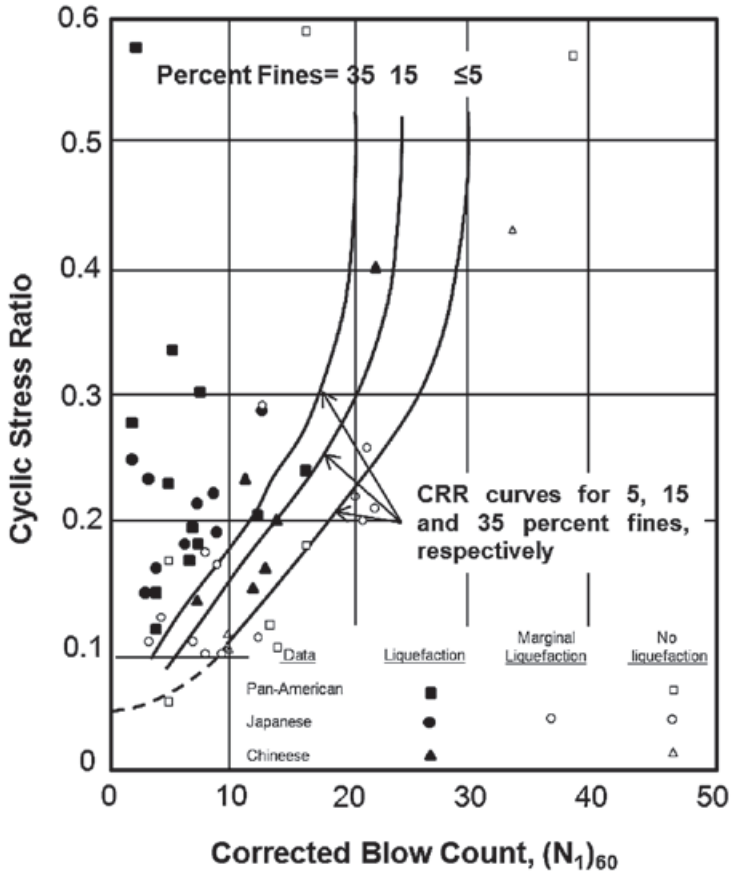

Figure 3. SPT Clean Sand base curve for magnitude 7.5 earthquakes with data from liquefaction case histories (Seed *et al.*, 1985).

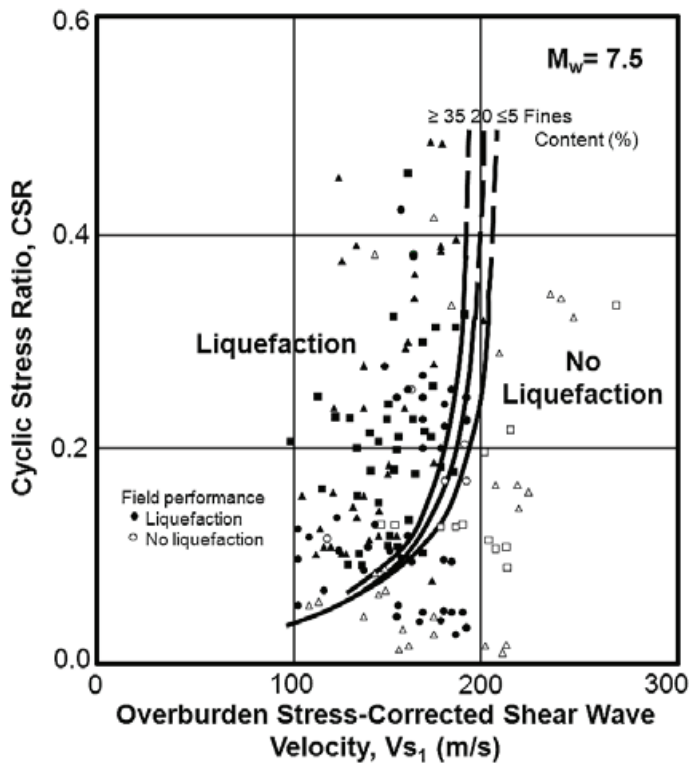

Figure 4. Liquefaction resistance curves by Andrus and Stokoe (2000) for magnitude 7.5 earthquakes and uncemented soils of Holocene age with case history data.

$$CRR = a\left(\frac{V_{S1}}{100}\right)^2 + b\left(\frac{1}{V^*_{s1} - V_{s1}} - \frac{1}{V^*_{s1}}\right) MSF \quad (4)$$

where V_{s1} was defined previously; MSF is the magnitude scaling factor for earthquakes with magnitudes different from 7.5 M_w; a, b are fitting parameters (a = 0.022, b = 2.8) and V^*_{s1} is a reference shear wave velocity that depends on the amount of fines present in the sand mass:

$V^*_{s1} = 200\ m/s$ soils with 35% fines.
$V^*_{s1} = 210\ m/s$ soils with 20% fines.
$V^*_{s1} = 215 - 220\ m/s$ soils with 5% fines.

The overburden stress correction is

$$V_{s1} = V_s\left(\frac{Pa}{\sigma'_v}\right)^{0.25} \quad (5)$$

where V_s is the measured shear wave velocity, (m/s); P_a is a reference stress (atmospheric pressure); σ_v is initial effective overburden stress, (kPa).

The magnitude scale factor MSF is used to translate the CRR vertically depending on the magnitude of the design or expected earthquake, i.e. MSF moves up or down the threshold for the occurrence of liquefaction given by CRR according to the size of the earthquake. It is given by:

$$MSF = \left(\frac{M_w}{7.5}\right)^{-2,56} \quad (6)$$

where M_W is the earthquake moment magnitude.

Field Tests

The field work presented in this paper forms part of geological and geophysical studies commissioned by local authorities after the April 4, 2010 event (Acosta Chang *et al.*, 2010). They obtained thirty seismic profiles from MAM and MASW tests during May and June 2010 at the Solidaridad Social Township. The fieldwork also included four geotechnical soundings to carry out SPT tests down to a depth of 11 m at the sites indicated in Figure 5. We used the seven seismic profiles closest to the SPT tests to compare and correlate the liquefaction potential estimated from both SPT blow counts $(N_1)_{60}$ and shear wave velocity (V_{s1}). Stratigraphic profiles were made at each SPT site to define the local geotechnical conditions and as a support for the geophysical interpretation. These field studies did not address the issue of assessing liquefaction

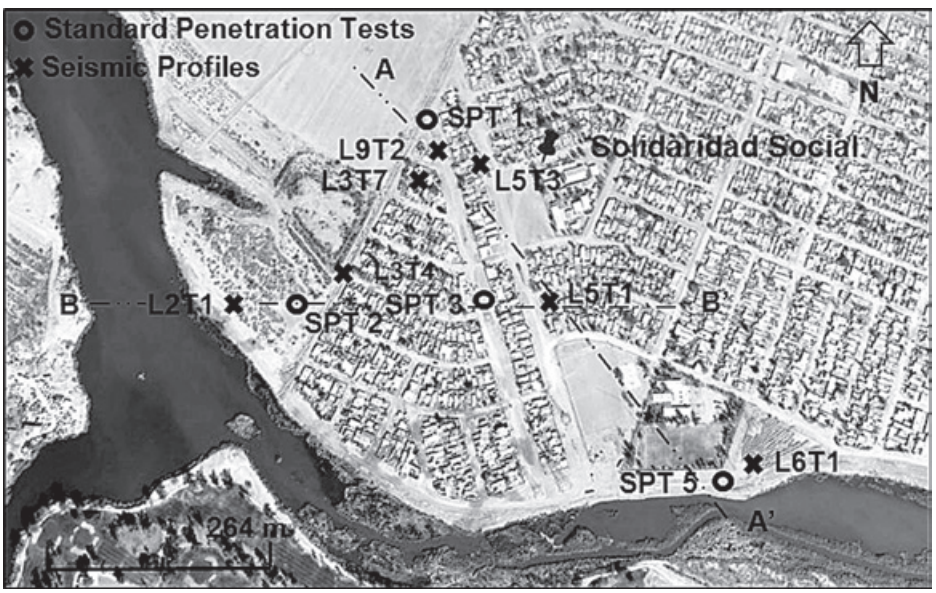

Figure 5. Location of seismic profiles and standards penetration tests (SPT) at the Solidaridad Social Township

potential.

MASW and MAM surveys were performed deploying twenty-four 2.5 Hz geophones along a linear array. Receivers were separated 1.5 m and were all connected to a multi-channel recording device.

The wave fields for MASW surveys were generated by vertical impacts of a 4.5 kg sledgehammer on a steel plate coupled to the ground. Sampling rate in the MASW surveys was 0.00125 s and records had a duration of 1 s. Seismic sources (impacts) were located at three positions collinear to the geophone array. The source positions are related to the position of the first geophone. For tests L2T1, L3T7, L5T3 and L6T1, the seismic source was located at the center of the line and the other two sources at both endes with a 1.5 m offset.

Three impacts were applied in succession at each position; records were collected, stacked and stored in a PC. Stacked records were used to achieve a single record associated with each position of the source to minimize the noise-signal ratio. In the case of seismic lines L3T4, L5T1 and L9T2 the spacing between geophones was 2.0 m.

Processing and partial results

MAM records were processed using Spatial Autocorrelation (SPAC), a well known technique to deduce a phase-velocity dispersion curve from microtremors recorded by a seismic array (Aki, 1957, 1965). The essence of the method is that, having records from seismic stations spaced at a constant distance and forming pairs of stations along different azimuths, it is possible to compute an estimate of the phase velocity of the waves crossing the array, without regard to the direction of propagation of the waves present.

If the duration of the MAM records obtained along a linear array is long enough, the recorded motion can be expected to include waves propagating along many different directions. Under this hypothesis, the equations and results that Aki (1957) obtained using the azimuthal average of the spatial cross-correlation coefficients can be applied (Chavez *et al.*, 2006). Having a linear array is also convenient because it allows for the collection of data using the same setup as in MASW, thus avoiding re-positioning of the geophones, a task that often requires significant additional field effort.

MAM data were acquired along the same linear array as in the MASW tests. The sampling interval was 2 ms and the duration of the records was 30 s. At least 30 background noise measurements were made at each seismic profile.

SPAC functions, $\rho(r, \omega)$ were defined by Aki (1957) in terms of the spatial autocorrelation of ground motion records separated a distance, r, represented as:

$$\rho(r,\omega) = J_o \left(\frac{\omega r}{c(\omega)} \right) \tag{7}$$

where $c(\omega)$ is the phase velocity associated to the frequency ω; J_0 is the Bessel function of first class and zero order.

SPAC functions were estimated in this study as the average value of the real part of the coherence function calculated between each pair of records obtained with the same spacing between geophones. Thus, the above process renders a SPAC function for each geophone spacing, 23 separations in this case. As an example we show Figure 6 that displays the real part of coherence function between all possible pairs of geophones in line L5T1, with an array size of 46 m. The separation between each geophone pair is plotted on the y-axis as distance and the SPAC functions on the x-axis.

SPAC functions contain information of seismic surface wave dispersion in which phase velocity can be measured as a function of frequency. The broken line in the figure joins the frequencies, F_{pcc}, associated to the first zero crossings of each calculated SPAC function. The value of F_{pcc} decreases as the separation between pairs of stations increases, up to a separation of 25 m, approximately.

Making reference to Figure 6, in the SPAC function associated with the separation of 2 m, one can measure the frequency associated with the first zero crossing, approximately 26 Hz. Because the argument of the Bessel function is, a phase velocity for 26 Hz is about 136 m/s, and 220 m/s for 3 Hz. This exemplifies how a different phase velocity is associated to each frequency.

Records from MAM surveys were transformed into the frequency-phase velocity space to form a dispersion image, using the Park *et al.*, (1999) method. The above process

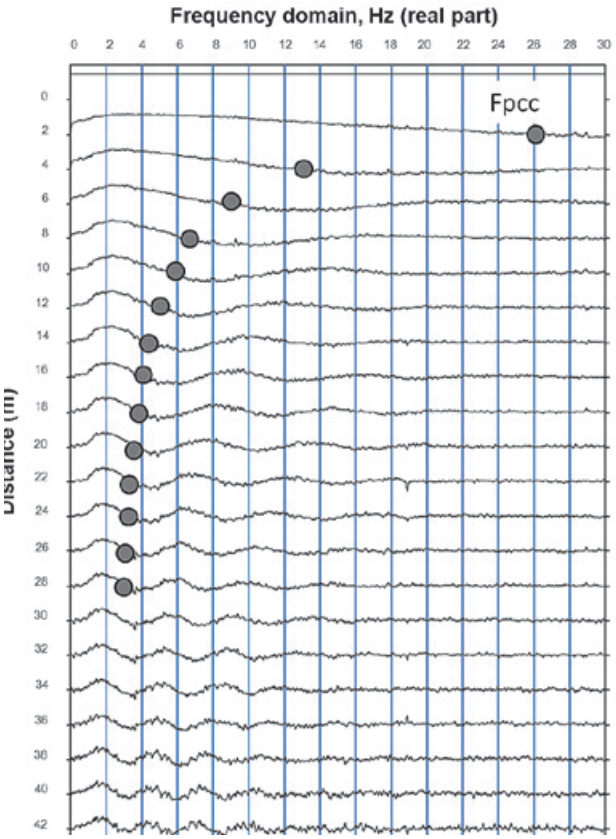

Figure 6. SPAC functions calculated for different separation distances between possible pairs of geophones. Dots represent the frequencies at the first zero crossing of each SPAC function.

is equivalent to the application of a 'slant stack' to the time signal. Dispersion curves from MASW surveys are obtained applying the same procedure except for the fact that they don´t use spatial autocorrelation. The graph in Figure 7 is a typical image that corresponds to line L5T1, with data collected for both MAM and MASW surveys.

The fundamental mode of surface waves for MAM records can be readily identified in Figure 7 in the 2-15 Hz frequency range and 6-29 Hz for the MASW records. The range of validity for both curves (passive and active) is limited by two straight lines having a constant wave length, 8 and 150 m as seen in Figure 7a. The Rayleigh wave fundamental mode of propagation is identified inside this range as a smooth curve formed by the maximum spectral energy with phase velocity decreasing with frequency (Park *et al.*, 1999).

The dispersion curves from the active and passive methods (MASW and MAM respectively) were combined to obtain a single dispersion curve covering a wider frequency range (2.5 to 29 Hz). As seen in Figure 7c, phase velocity reduces sharply in going from 3 to 7 Hz and thereafter it reaches a constant value equal to 130 m/s. Both curves have approximately the same shape and actually overlap between 6 and 16 Hz.

Dispersion curves (phase velocity-frequency) and the inversion of shear wave velocity (V_s) profiles were obtained using the procedure described in the SeisImager/SW software manual (Geometrics, 2006). The SeisImager inversion technique is a deterministic method that depends on an initial model in which shear velocity increases with depth and in which the least square inversion is then applied (Xia, 1999b).

The initial shear wave velocity model is generated from the information provided by the phase velocity curve assuming that penetration depth is about one third of the wave length associated to each of the measured phase velocities. The procedure considers *n-1* layers with a constant thickness; the *nth* layer is twice as thick. In our calculations we used seven layers and, starting from the initial model, proceeded on to the nonlinear iterative inversion procedure.

Figure 8 shows the dispersion curves combining the results of MASW and MAM surveys for the Solidaridad Social Township. We estimated shear wave velocity (V_s) profiles

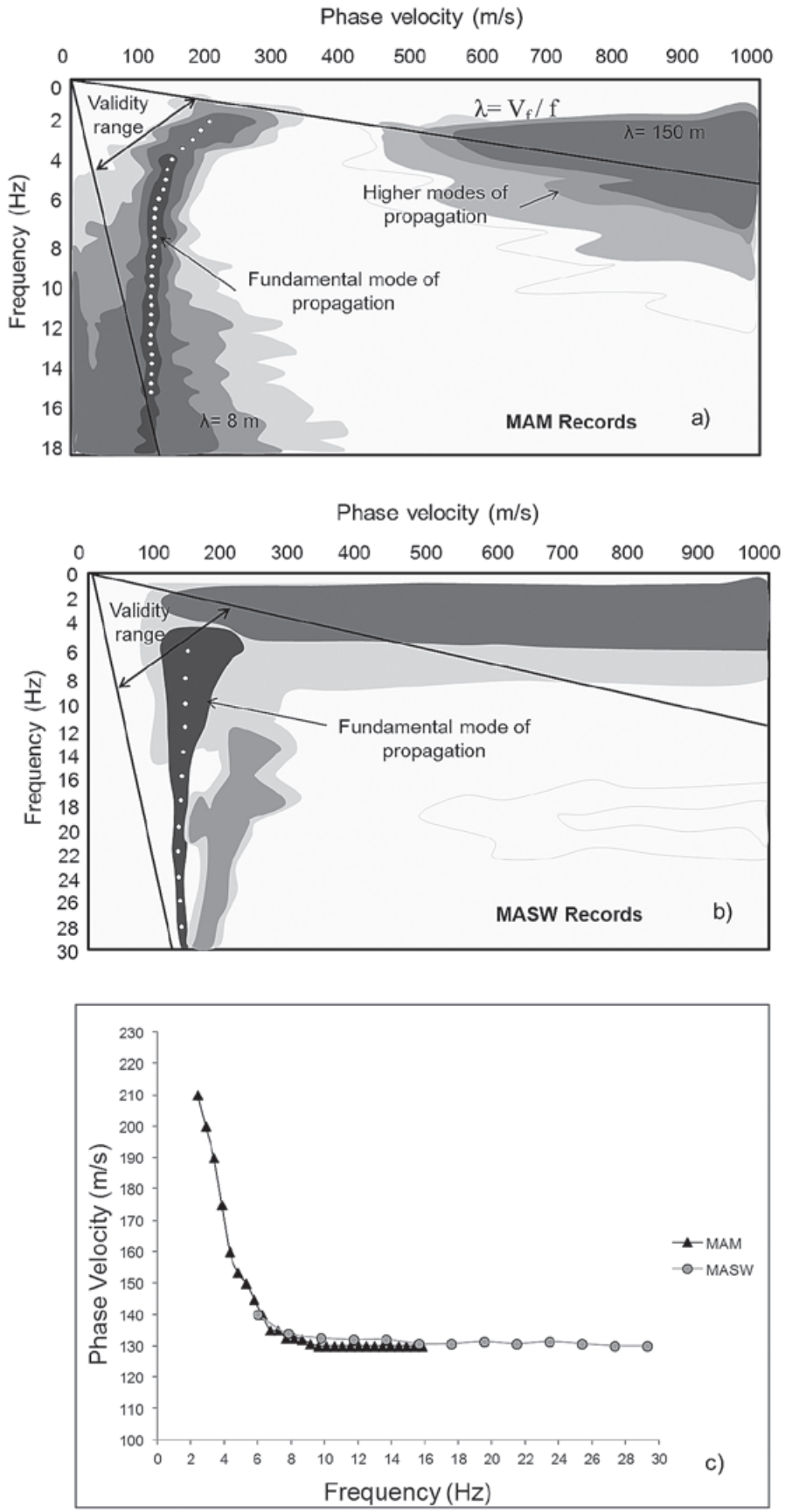

Figure 7. (a) The phase velocity-frequency image of MAM records. (b) The phase velocity-frequency image of MASW records and (c) Dispersion curves for active MASW and for passive MAM corresponds to the line L5T1.

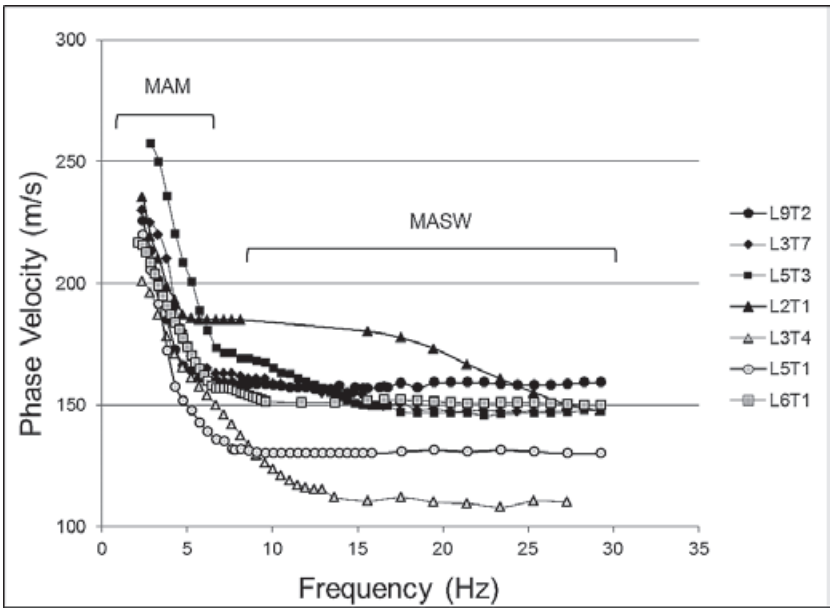

Figure 8. Dispersion curves combining MASW and MAM techniques.

Table 1. Seismic Units

Seismic Units	Seismic Profiles (m/s)						
	L9T2	L3T7	L5T3	L2T1	L3T4	L5T1	L6T1
1 (3.5 -10 m)	174	170	165	-	125	135	162
2 (10- 17 m)	164	164	189	188	196	157	161
3 (17- 26 m)	212	212	229	198	189	208	241
4 (26- 30 m)	268	312	312	278	226	241	218

at depths varying from 1.8 up to 30 m (figure 9), approximately. In this specific case the method stops being reliable at depths larger than 30 m.

Results

The graphs in Figure 9 show the shear wave velocity profiles obtained from the MASW and MAM dispersion curves. This information has been summarized in Table 1. Regarding liquefaction potential, there are four significant seismic units:

Unit 1. It goes from about 3.5 to 10 m in depth. Shear wave velocities vary from 125 to about 174 m/s; lowest values were found in L5t1 and L3T4, located close to the location of soundings SPT 3 and SPT 2, respectively (see Figure 5). Shear wave velocities en line L6T1, close to SPT 5, were about 162 m/s. Values in the remaining three lines, L9T2, L3T7 and L5T3 average 170 m/s.

Unit 2. It goes from 10 to 17 m in depth. Shear wave velocities in lines L9T2, L3T7, L5T1 and L6T1 are about 160 m/s and around 185 m/s in lines L5T3 and L2T1 and slightly larger in line L3T4.

Unit 3. Shear wave velocity values in this unit are scattered within the 189 to 241 m/s range, in depths that go from 17 to 26 m.

Unit 4. Shear wave velocity is more widely scattered in this unit, varying from 218 to 312 m/ s at depths that go from 26 m down to the maximum depth monitored with our dispersion curves, 30 m.

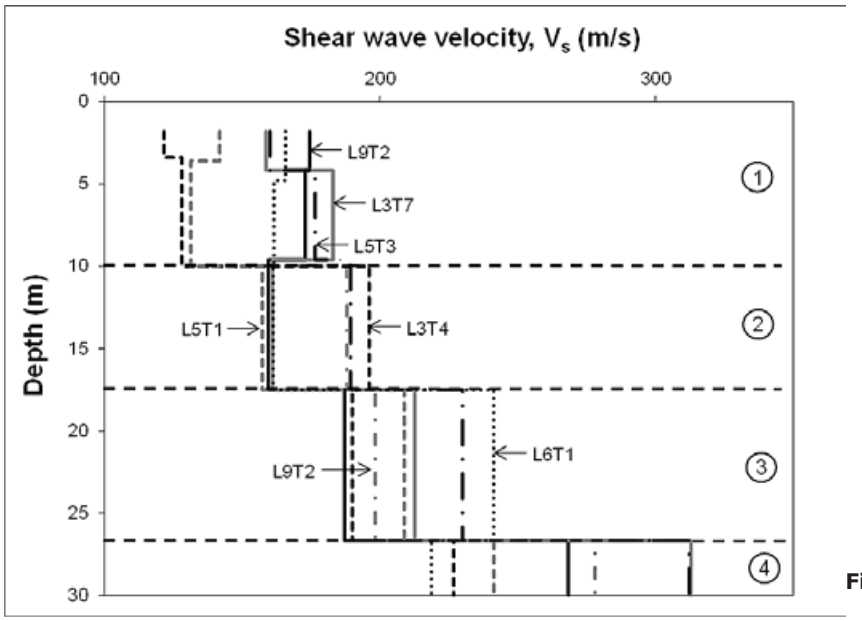

Figure 9. Shear Wave Velocity Profiles

The shallowest strata cannot be identified from MAM/MASW measurements, as the dispersion curve cannot be reliably estimated for frequencies above 1.9 Hz due to the spatial aliasing limit. As seen in figure 10, the upper most strata are clayey soils reaching depths of as much as 2 m. These clays are not liquefiable; their presence hinders the dissipation of pore pressures and enhances the formation of sand boils when the underlying sandy soils liquefy. Water table was located about 10 m below the surface at sounding SPT1 but is much shallower at the other sites, 3 to 5 m.

Penetration resistance of these sandy soils is seldom larger than 20 blows and applying the simplified method (equations 1 to 3) from the blow counts obtained from soundings SPT 1, SPT 2, SPT 3 and SPT 5, their high potential for liquefying was ratified. In applying equation 1, the value of a_{max}= 0.23 g was taken from the maximum ground acceleration recorded at the Tamaulipas station during the El Mayor-Cucapah event. The epicentral distance between our study site and the Taumalipas station is approximately the same for the El Mayor-Cucapah earthquake. The clean sand CRR curve in figure 2 [CRR-$(N_1)_{60}$] applies only for earthquakes with a magnitude equal to 7.5. We used the I.M Idriss (1997) correction factors to scale down the CRR curve to magnitude 7.2 as in the April 4, 2010 earthquake, following the recommendations of the NCEER workshop (Youd, et al., 2001). We also performed analyses assigning a larger a_{max} value (=0.45 g), as recommended in the Civil Engineering Design Manual from the Mexican electricity board (CFE, 2008) and also included a complementary analysis with a_{max}= 0.35 g. Figure 11, show that the ground below the water level is potentially liquefiable for the three maximum accelerations used in the al analyses to the maximum depth explored with the SPT soundings.

Liquefaction potential was also assessed from the shear wave velocity profiles shown in Figure 12 and obtained from the MAM and MASW surveys. Maximum ground acceleration values and correction factors to scale down the CRR curve of Figure 4 to a 7.2 magnitude were the same as those used in the SPT analyses.

The stratigraphical interpretation of the seismic profiles can only be done down to the maximum explored depth in the SPT soundings, 11 m, as shown in Figure 10. It is to be expected that deeper strata are also sands or sandy non plastic soils, as can be inferred from the shear wave velocity values obtained form MAM and MASW surveys and from the geological and physiographical conditions at the Solidaridad township (Jaime A., 1980). These sandy soils having shear wave velocities of less than about 200 m/s are also liquefiable, according to our analyses. However, a vast number of past experiences have shown that liquefaction seldom occurs at depths larger than about 20 m (Seed and Idriss, 1971; Ovando and Segovia, 1996; YU S., Tamura M. and Kouichi H., 2008).

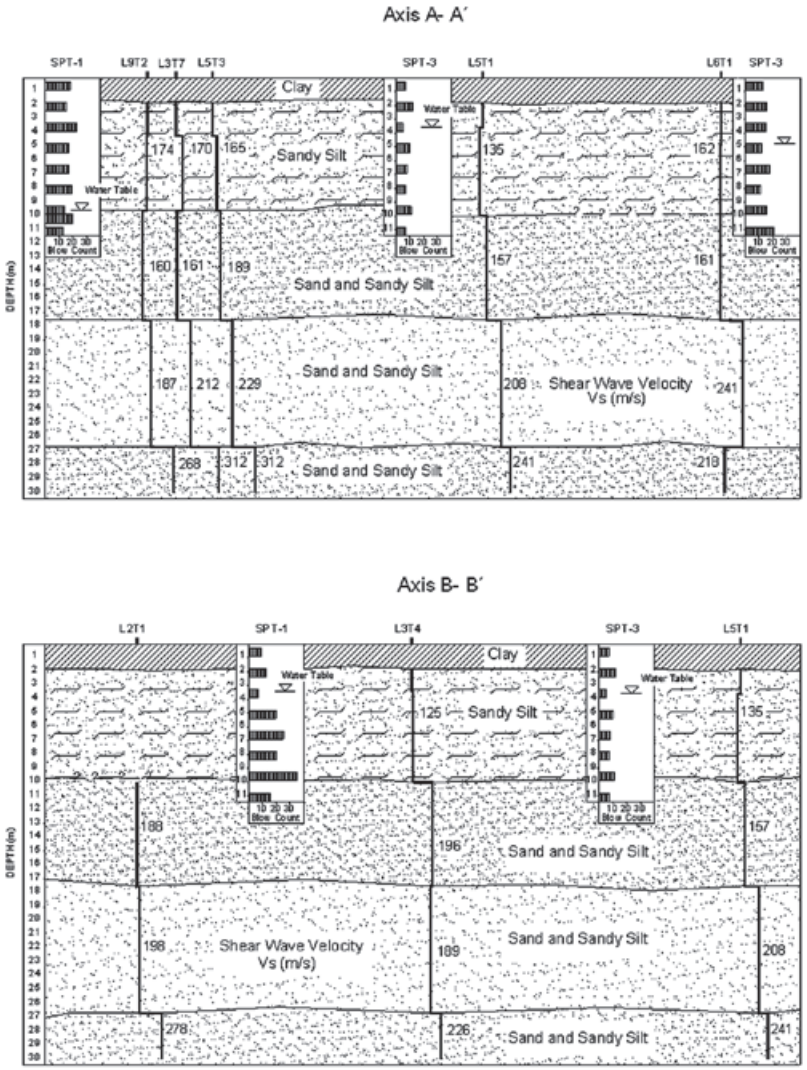

Figure 10. Stratigraphy of the Solidaridad Social Township

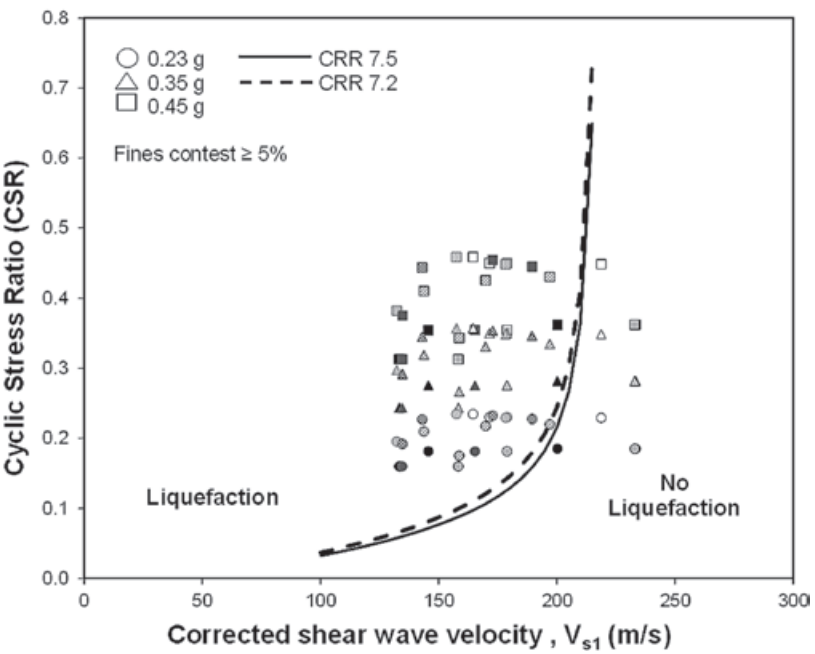

Figure 11. Curve for calculation of CRR versus $(N_1)_{60}$

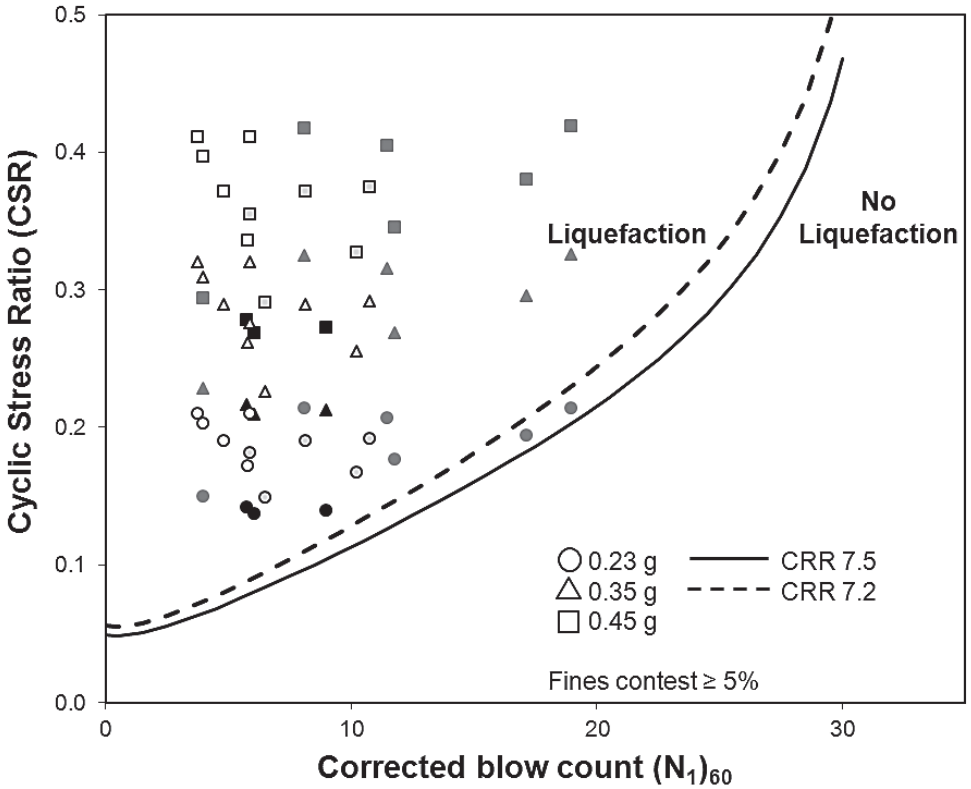

Figure 12. Curve for calculation CRR versus V_{s1}

Shear velocity profiles obtained from all the MAM and MASW measurements were plotted in a single graph, Figure 13 (see also Table 1). Results show that the lowest shear wave velocities in sandy soils were obtained in lines L3T4 and L5T1, which have the highest risk of liquefaction. Overall, sand strata between depths 5 and 17m are highly prone to liquefy again for earthquakes inducing peak ground accelerations of at least 0.23 g and M_w magnitudes of 7.2. Strata between 17 and 25 m may also liquefy but are not as susceptible. Liquefaction potential analyses using SPT blow counts and V_s are equivalent in that both yielded the same results.

Having established CRR, a factor of safety against liquefaction can be determined for each CRR value at any depth, as a function of V_{s1}.

According to this, liquefaction will occur whenever that factor is less than unity. Making it equal to 1 and substituting values in equations 1 to 6, we estimated the minimum values of shear wave velocity (critical shear wave velocity, V_{sc}) required to bring about liquefaction, for different peak ground accelerations, a_{max}, assuming the same earthquake magnitude, M_w = 7.2.

The plots of Figure 14, a_{max}, against V_{sc}, define two trend lines that characterize two zones in the Solidaridad Social Township. The first one represents data obtained from seismic profiles L9T2, L3T7 and L5T3, that are all clustered around the geotechnical sounding SPT 1 in a zone where the water table is rather low (9.6 m). The second trend line includes the rest of the seismic profiles at locations near the standard penetration tests SPT 2, SPT 3 and SPT 5. Water table in these sites is higher, between 3.4 to 4.8 m, since they are closer to the riverbank. Data in the figure demonstrate that, given a value of V_{sc} sites near the riverbank will liquefy with lower a_{max}, values than the sites clustered around SPT-1. This illustrates the manner in which groundwater influences liquefaction susceptibility, it decreases with increasing water table depth, that means under these conditions no liquefaction will take place in the superficial layers as they dry out or become partially saturated. Groundwater level is not stationary; so seasonal variations can alter the vulnerability of sand strata to liquefaction, especially in the uppermost soil layers.

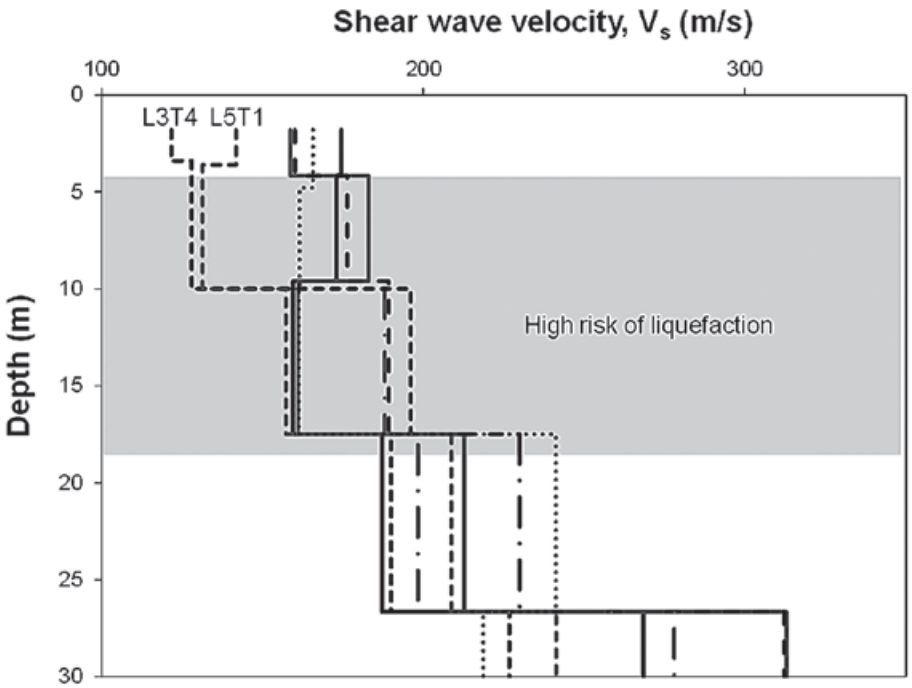

Figure 13. Geotechnical characterization of the subsoil at Solidaridad Social Township

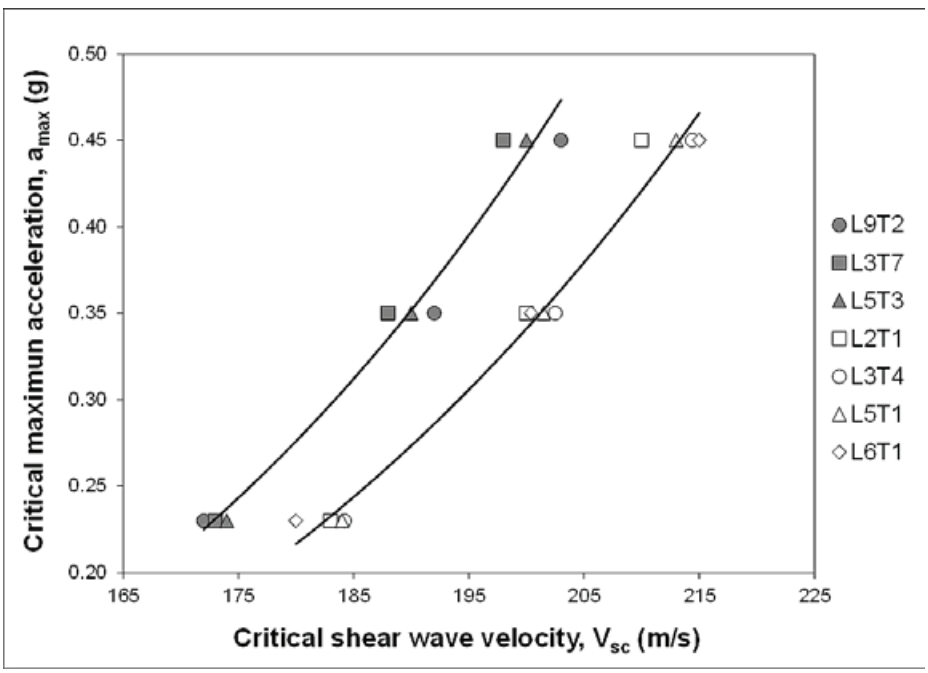

Figure 14. Trend lines of the Solidaridad Social Township

Conclusions

Results presented in this paper showed that the combination of active and passive methods (MAM and MASW) is a viable and low cost procedure to obtain reliable shear wave velocity profiles in urban environments. Our shear wave velocity profiles were derived from 30 m deep seismic lines that were utilized to obtain shear wave velocity profiles form MAM and MASW records and then to evaluate the liquefaction potential of the sandy soils at a site in the Solidaridad Social Township, 5 km south of the city of Mexicali.

Liquefaction potential was estimated for the April 4, 2010 earthquake using a well known simplified empirical procedure adapted to be

used in terms of shear wave velocity values. In our simplified liquefaction analyses we used an a_{max}, value recorded at a nearby station and the actual Mw magnitude of the 2010 event. We also performed complementary analyses with two other a_{max} values.

Geotechnical soundings were also performed after the El Mayor-Cucapah event and we also used the results of SPT sounding to assess liquefaction potential; we compared these results with those obtained applying the simplified empirical procedure from the seismic profiles we obtained with the MAM/MASW shear wave velocity profiles. Our results showed that both analyses are equivalent.

The procedure we presented and discussed has evident advantages over traditional methods for assessing the potential for sand liquefaction as it does not require geotechnical boreholes (SPT or CPT soundings) nor does it need drilling of boreholes to carry out field tests to obtain shear wave velocity profiles from conventional geophysical profiling methods (up-hole, down-hole or cross-hole tests). The instruments for measuring vibrations in MAM or MASW surveys are standard geophones and analysis of vibration records is relatively simple.

The liquefaction potential analyses presented here pointed out that the soils will liquefy again, should another large earthquake hit the region. Successive liquefaction events in the same site have been known to occur in the past and are not uncommon.

Finally, it must be emphasized that effective characterization of soil deposits may require the use of several seismic profiling methods in order to obtain suitable information to sufficiently understand relevant subsurface conditions for a particular project or situation.

Bibliography

Acosta Chang J.G., Vásquez S., Mendoza L.H., Hernández F., Salas J., Ruiz e., Arellano g., R. Reyes R., Granados O., 2010, Estudio geofísico y geológico en la colonia Solidaridad Social, Mexicali Baja California. *Informe técnico para el Ayuntamiento de Mexicali. pp. 107 (Registro CICESE PA: 101086)*

Aki K., 1957, Space and time spectra of stationary stochastic waves, with special reference to microtremors. *Bulletin of the Earthquake Research Institute, 35, 415-456.*

Aki K., 1965, A note on the use of microseisms in determining the shallow structures of the earth's crust. *Geophysics, 30, 665-666.*

Andrus R.D., Stokoe K.H., 1997, Liquefaction resistance based on shear wave velocity", NCEER Workshop on evaluation of liquefaction resistance of soils. *Technical Report NCEER-97-0022, T. L. Youd and I. M. Idriss, Eds., held 4-5 January 1996, Salt Lake City, UT, National Center for Earthquake Engineering Research, Buffalo, NY, 89-128.*

Andrus R.D., Stokoe, K.H., 2000, Liquefaction resistance of soils from shear-wave velocity. *Journal of Geotechnical and Geoenvironmental Engineering, ASCE, 126 (11),1015-1025.*

Centro de Investigación Científica y de Educación Superior de Ensenada B.C, http://ranm.cicese.mx/, consulta noviembre 2013.

Chavez-Garcia F.J., Rodriguez M., W. R. Stephenson, 2006, Subsoil Structure Using SPAC Measurements along a Line. *Bulletin of the Seismological Society of America, 96 (2), 729–736.*

Ishihara K., 1993, Liquefaction and flow failure during earthquakes. *Geotechnique, 43 (3): 351-415*.

Jaime A., 1980, Comportamiento dinámico de suelos, X Reunión Nacional de Mecánica de Suelos, 92-94, Morelia, Michoacán.

Kayen R., Mitchel J., Seed R., Lodge A., Nishio S., Coutinho R., 1992, Evaluation of SPT-CPT and shear wave-based methods for liquefaction potential assessment using Loma Prieta data, Proceeding 4th Japan-US workshop on Earthquake, 177-204, Honolulu, HI, May 27-29.

Liao S., Veneziano D., Whitman R., 1988, Regression models for evaluating liquefaction probability. *Journal of Geotechnical Engineering, ASCE, 114 (4), 389-409.*

Ludwig W.J., Nafe J.E., Drake, C.L., 1970, Seismic refraction, in The Sea. Wiley-Interscience, New York, 53-84 pp.

Manual design of civil works, 2008**,** Design by earthquake. Recommendations and Comments, Federal Electricity Commission (CFE), Distrito Federal, Mexico.

Marchetti S., Monaco P., Totani G., Calbrese M., 2001, The flat dilatometer test (DMT) in soil investigations", A report by the ISSMGE committee TC16, Proceedings IN SITU 2001, International Conference on in situ measurement of soil properties, 44, Bali, Indonesia.

Marcuson W.F., 1978, Definition of Terms Related to Liquefaction. *Journal of Geotechnical Engineering Division, ASCE, 104 (9), 1197-1200*

Ovando E. y Segovia P., 1996. Licuación de arenas. TGC Geotécnia S.A de C.V.

Park C., Miller R., Xia J., 1999, Multichannel analysis of surface waves. *Geophysics, 64, 800-808.*

Park C.B., Miller R.D., Xia J., Ivanov J., 2007, Multichannel analysis of surface waves (MASW)-active and passive methods. The Leading Edge (TLE), 26 (1), 60-64.

Poulos S.J., Castro G., France W., 1985, Liquefaction evaluation procedure. *Journal of Geotechnical Engineering Division, ASCE, 1 (6), 772-792.*

Robertson P.K., Wride C.E, 1998, Evaluating cyclic liquefaction potential using the Cone Penetration Test. *Canadian Geotechnical Journal, 35(3), 442-459.*

Seed H.B., 1979, Soil liquefaction and cyclic mobility evaluation for level ground during earthquakes. *Journal Geotechnical Engineering Division, ASCE, 105, 210- 255.*

Seed H.B., Idriss I.M., 1982**,** Ground motions and soils liquefaction during Earthquakes. *Earthquake Engineering Research Institute Monograph, Oakland, California.*

Seed H.B., Tokimatsu K., Harder L.F., Chung R.M., 1985, Influence of SPT procedures in soil liquefaction resistance evaluations. *Journal of Geotechnical Engineering, ASCE, 111 (12), 1425-1445.*

Seed H.B., Idriss I.M, 1971, Simplified procedure for evaluating soil liquefaction potential. *Journal of the Soil Mechanics and Foundation Division, ASCE, 97 (9), 1249-1273.*

Seed H.B., Idriss I.M., Arango I., 1983**,** Evaluation of liquefaction potential using field performance data. *Journal of Geotechnical Engineering, ASCE, 109 (3), 458-482.*

Stokoe K.H, Narzian S., 1985, Use of Rayleigh waves in liquefaction studies, Measurements and use of shear wave velocity for evaluating dynamic soil properties. Geotechnical Engineering Division, ASCE, 1-17.

Tokimatsu K., Uchida A., 1990, Correlation between liquefaction resistance and shear wave velocity. *Soils and foundations, Japanese Society of Soil Mechanics and Foundation Engineering, 30 (2), 33-42*.

Xia J., Miller R.D., Park C.B., 1999b, Estimation of near-surface shear-wave velocity by inversion of Rayleigh wave. *Geophysics, 64, 691-700.*

Youd T.L., Idriss I.M., 2001, Liquefaction resistance of soils: Summary Report from the 1996 and 1998 NCEER/NSF Workshops on evaluation of liquefaction resistance of soils. *Journal of Geotechnical and Geoenvironmental Engineering, ASCE, 127, Nº AISSN 1090-0241.*

YU S., Tamura M., Kouichi H., 2008**,** Evaluation of liquefaction potencial in terms of surface wave method, The 14 th Worl Conference on Earthquake Engineering, Beijing, China.